RESEARCH ARTICLE

Sustainable Nanocellulose-PEO Composites Reinforced with Functional Nanofillers in High-Performance Dielectric Nanocomposites for Green Flexible Electronics

Gitanjali Jothiprakash[1], Dongyang Sun[1,*], Peter Adonteng[1], Chan Hwang See[1], Elsa Lasseuguette[1], Zhilun Lu[2], Ramesh Desikan[3], Subburamu Karthikeyan[3] and Senthilarasu Sundaram[4]

[1] School of Computing, Engineering & Built Environment, Edinburgh Napier University, Edinburgh EH10 5DT, United Kingdom
[2] Faculty of Engineering and Physical Sciences, University of Leeds, Leeds LS2 9JT, United Kingdom
[3] Agricultural Engineering College and Research Institute, Tamil Nadu Agricultural University, Coimbatore, Tamil Nadu, 641003 India
[4] School of Computing, Engineering and Digital Technologies, Teesside University, Middlesbrough TS1 3BX, United Kingdom

Abstract

The growing demand for sustainable materials in green flexible electronics calls for alternatives to petroleum-derived polymers, which are non-biodegradable, resource-intensive, and environmentally harmful. This study presents the fabrication of bio-composite films using water hyacinth derived cellulose nanofibrils (CNF), blended with polyethylene oxide (PEO) and reinforced by functional nanofillers such as barium titanate (BTO), silver nanowires (SNP), and carbon nanotubes (CNT). The nanocomposite films (NCF) were produced by solution casting and systematically characterized for morphological, dielectric, mechanical, thermal, and chemical properties. Scanning electron microscopy analysis revealed well-dispersed CNF (-30 nm diameter) uniformly embedded within a CNF/PEO matrix and nanofillers (0.5–2%). Dielectric testing showed that BTO significantly enhanced permittivity (>200), making it promising for capacitor and antenna applications, although dielectric loss increased at higher nanofiller loadings. SNP-reinforced NCF exhibited moderate permittivity (50–90) but higher dielectric loss (0.15–0.32), supporting multifunctional applications requiring both dielectric and conductivity. CNT reinforced with NCF provided a balanced performance, with stable permittivity, relative low dielectric loss (< 0.015) and superior mechanical flexibility. Mechanical testing confirmed that BTO increased stiffness and tensile strength (1.5–2%), SNP enhanced strength but reduced ductility up to 1.5%, and CNT offered reinforcement at 1.5% with preserved elongation (up to 6%). FTIR spectra indicated strong interfacial interactions between nanofillers and CNF-PEO matrix. Thermal analysis revealed that CNT disrupted the crystalline structure of the matrix, lowering melting and crystallization temperatures, whereas BTO and SNP had negligible thermal effects. This study demonstrates a sustainable pathway to valorize an invasive species into a biodegradable, high-performance NCF for sustainable electronics, signifying a pathway toward flexible antenna, sensors, and energy storage materials.

Submitted: 28 September 2025
Accepted: 15 October 2025
Published: 29 November 2025

Vol. 1, **No.** 1, 2025.
10.62762/JAEM.2025.761770

***Corresponding author:**
✉ Dongyang Sun
D.Sun@napier.ac.uk

Citation
Jothiprakash, G., Sun, D., Adonteng, P., See, C. H., Lasseuguette, E., Lu, Z., Desikan, R., Karthikeyan, S., & Sundaram, S. (2025). Sustainable Nanocellulose-PEO Composites Reinforced with Functional Nanofillers in High-Performance Dielectric Nanocomposites for Green Flexible Electronics. *Journal of Advanced Electronic Materials*, 1(1), 5–16.

Keywords: cellulose, nanofibrils, nanocomposite films, sustainable materials, water hyacinth.

1 Introduction

The development of green electronics highlights the serious requirement to develop sustainable materials that reduce the impact on environment associated with conventional electronic manufacturing [1]. Conventional electronics depend on non-biodegradable, petroleum-based polymers that significantly contribute to toxic chemical pollution, e-waste, and exhaustion of non-renewable resources [2]. The lifecycle of this kind of materials, from production to disposal, poses high environmental risks, with landfill waste and release of toxic gases during degradation or incineration. This has led to increased research on biopolymer-based composites that are biodegradable, renewable, and hold the essential mechanical and electrical properties for high-performance, durable electronics [3].

Among renewable resources, water hyacinth (Eichhornia crassipes), is a globally invasive aquatic plant, has emerged as a promising alternative raw material due to its rapid proliferation, high cellulose, and low lignin content, which simplifies nanocellulose extraction compared to conventional feedstock. Water hyacinth (WH) has 23-57% cellulose content, enabling substantial nanocellulose yield via optimized extraction methods. Nanocellulose synthesized from water hyacinth exhibits high crystallinity index (85%), nanoscale dimensions (10–30 nm in diameter), biodegradability, high tensile strength, and low toxicity. It makes a water hyacinth material as an attractive reinforcing biopolymer intended for green electronic applications [4, 5]. At the nanoscale, cellulose fibrils act as dielectric filler that generates numerous interfaces and polarization sites within a polymer matrix. This interfacial Maxwell-Wagner-Sillars polarization enables charge accumulation at nanocellulose-polymer-nanoparticle boundaries, enhancing relative permittivity particularly at low frequencies where dipole orientation is equilibrated. Such interfacial effects are critical in designing bio-based nanocomposites with tailored dielectric properties for electronic applications [6].

Extraction of nanocellulose from water hyacinth typically involves sequential chemical and mechanical treatments: bleaching with sodium hypochlorite to remove lignin, alkaline hydrolysis to eliminate hemicellulose, and acetic acid hydrolysis to separate crystalline cellulose domains. Mechanical methods such as high-pressure homogenisation or ultrasonication further disperse fibrils into colloidal suspensions, yielding materials with high crystallinity, surface area, and thermal stability [7, 8]. Optimization of process parameters, such as hydrolysis time and temperature, has enabled in CNC yields exceeding 70%, supporting economically viable for scaling up [9].

Blending the nanocellulose fibers into polyethylene oxide (PEO), a biocompatible and flexible synthetic polymer, produces hybrid composites that couple the strength and sustainability of nanocellulose with the processability of PEO. The addition of functional nanoparticles viz., barium titanate (BTO), silver nanowires (SNP), and carbon nanotubes (CNT), further tailors the composites by enhancing dielectric constant, thermal stability, and electrical conductivity. BTO contribute ferroelectric behaviour, improving permittivity crucial for antenna and energy storage applications, while CNT and SNP enhance mechanical robustness, and charge transport, meeting the requirement of lightweight, flexible, and green electronic devices [10, 11]. This bio-composite will enable application across low-frequency and high-frequency electronic devices as depicted in Figure 1.

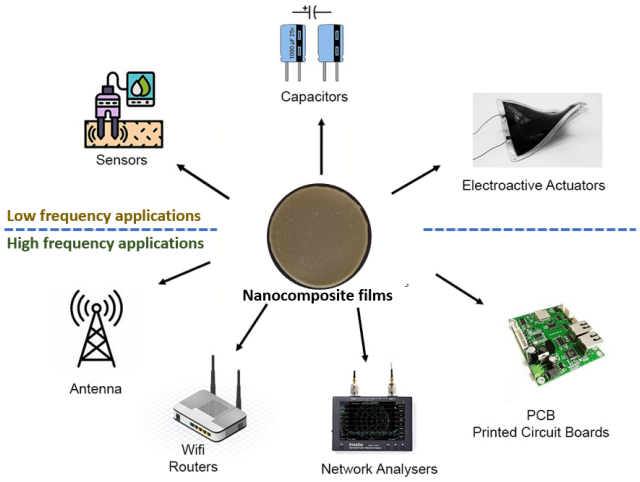

Figure 1. Applications of nanocomposite across electronic devices.

This integration of WH-derived nanocellulose, PEO polymer, and dielectric nanoparticles simultaneously valorises an invasive ecological species and generates biodegradable, high-performance bio-composite suited for next-generation sustainable electronics. By lowering reliance on non-renewable feedstock, lowering environmental issues, and allowing green devices such as antennas, energy storage materials and

sensors, this approach fuses ecological remediation with developments in materials science, showing a pathway toward scalable, ecofriendly aligned electronics [12–14].

2 Materials and Methods

2.1 Preparation of Nanocomposite Films

Fresh water hyacinth (WH) stems were collected, washed thoroughly, dehydrated, and pulverised to a particle size of 1-2 mm. Cellulose extraction was carried out through sequential chemical treatments: (i) bleaching in sodium hypochlorite (NaClO, pH 4) overnight to remove lignin, (ii) alkaline hydrolysis in sodium hydroxide (NaOH, 1 %) for 2 h to eliminate hemicellulose and residual lignin, and (iii) a second NaClO bleaching step for 2 h. After each step, the material was washed with ultrapure water by centrifugation and decantation. The purified cellulose was converted into cellulose nanofibrils (CNF) using PSI-20 high-pressure homogeniser [15]. CNF and PEO polymers were used as the biopolymer matrix components. The PEO polymer (Mv:100,000), and the functional nanofillers, barium titanate (BTO) [cubic nanopowder, 50 nm], silver nanowires (SNP) [50 nm $\times$ 6 μm, 0.5% IPA suspension] and carbon nanotubes (CNT) [multi-walled, 6-13 nm $\times$ 2.5-20 μm], were acquired from Sigma-Aldrich with high purity (>99%) and used without further modification.

Nanocomposite films (NCF) were prepared by solution casting method as illustrated in Figure 2. CNF and PEO were dissolved in an ultrapure water to form a polymer blend of 1:2 weight ratio and stirred for 20 minutes at 60°C. The nanofillers were dispersed in the solution at varying weight concentrations (0.5%, 1%, 1.5%, and 2%) with respect to total CNF and PEO content. The dispersions were obtained using PSI-20 high-pressure homogenizer for 10 minutes to ensure homogeneous distribution of nanofillers within the matrix of polymer. The solutions were casted onto new glass petri dish and dried at 40°C to form films. Films without nanofillers were also prepared under the same conditions for comparison as control film. The dried films were peeled and conditioned at ambient condition before characterization.

2.2 Characterization of Nanocomposite Films

The surface morphology of the NCF was examined using a field-emission scanning electron microscope (FE-SEM, Hitachi S-4800, Japan). Samples were cut into approximately 1 × 1 mm pieces and dried overnight at ambient temperature prior to analysis.

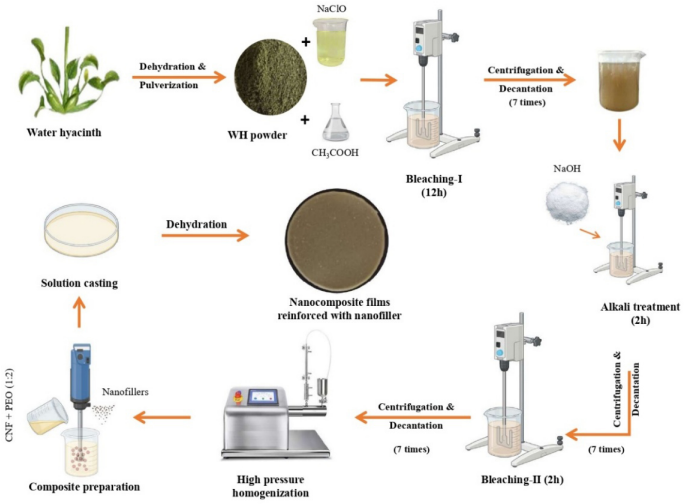

Figure 2. Preparation of nanocomposite films reinforced with nanofillers.

Each specimen was sputter-coated with a thin gold layer for 120 s using an EMITECH K550X coater (Quorum Technologies, UK) to minimize charging effects. Imaging was conducted at an accelerating voltage of 3 kV under various magnifications to capture the microstructural features.

Low-frequency dielectric properties were measured using a precision LCR meter (Keysight E4980A) over 1 kHz to 1 MHz at ambient temperature. Square film samples were coated with silver paint electrodes on both sides and placed between parallel plates. Film thickness and electrode area were measured for permittivity calculations. High-frequency dielectric properties were assessed using a split-post dielectric resonator (SPDR) system (QWDE, Poland), coupled to a vector network analyser [16, 17]. The film thickness was controlled with an accuracy of $\pm$0.01 mm. Samples were mounted in the SPDR cavity without air gaps, and the quality factor (Q) and resonant frequency (f) were recorded.

The tensile properties of the NCF reinforced with nanofillers were tested using a universal testing machine (Zwick UK) following the standard ASTM D882 standard. The tensile strength and elongation at break were analysed for three replicates of rectangular test strip of NCF and compared against control films. The functional groups of NCF were determined with FTIR spectrophotometer (Spectrum 100, Perkin-Elmer, UK) in the 4000-450 cm^{-1} range at 4 cm^{-1} resolution.

The thermal behaviour of the NCF reinforced with nanofillers was characterized using a differential scanning calorimeter (PerkinElmer 8000; Perkin Elmer UK, Buckinghamshire, UK). The sample weight of

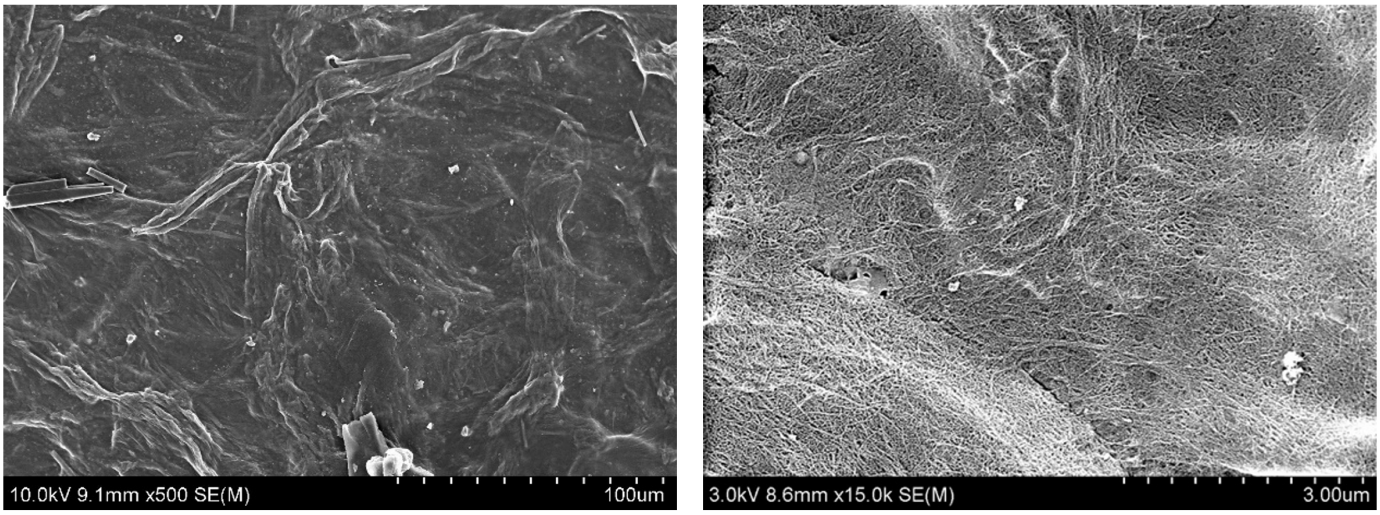

a. Low Magnification b. High Magnification

Figure 3. SEM micrograph of CNF-PEO films at (a) low and (b) high magnification.

~10 mg was kept in stainless steel pan and subjected to heating (-50°C to 200°C) at a rate of 10°C/min to evade oxidation under a constant gas purge (Nitrogen gas: 20 mLmin^{-1}). A heating (two-cycle) protocol was used, the first heating overlapped prior thermal history, followed by cooling (up to -50°C) and a subsequent reheating (up to 200°C). In the second heating cycle, melting temperature (T_m), crystallization temperature (T_c), and allied enthalpy changes from the thermograms were determined.

3 Results and Discussion

3.1 Morphological Characterization

Representative SEM micrographs of the NCF-PEO (1:2 weight ratio) are shown in Figure 3. At low magnification (Figure 3a), a dense and interconnected fibrillar network is observed, in which cellulose fibrils appear well embedded within the PEO matrix. The fibrils exhibit a range of diameters and random orientations, forming a three-dimensional entangled structure that is uniformly filled by the polymer phase, consistent with previous reports of fiber–polymer hybrid films [18]ent of fibrils. Such surface roughness may influence the dielectric performance by enhancing interfacial polarization effects at the polymer-fibril interfaces [19].

At higher magnification (Figure 3b), individual cellulose nanofibrils with diameters of approximately 30 nm are clearly visible, forming elongated and interconnected thread-like domains. The presence of such fine and continuous nanofibrils is known to contribute significantly to the stiffness and tensile strength of cellulose-based composites [20]. This structural feature is therefore considered a major contributor to the mechanical reinforcement observed in the films.

NCF containing BTO, SNP and CNT (0.5–2 %) displayed morphologies similar to the control CNF-PEO matrix, with no distinct nanoparticle agglomerates visible under SEM at the magnifications used. This indicates that the nanofillers were well dispersed and embedded within the fibrillar-polymer network. Although SEM cannot directly confirm interfacial adhesion, the absence of phase separation or aggregation suggests favourable compatibility. Previous studies have highlighted that homogeneous nanofiller dispersion and strong matrix-filler interactions are essential in achieving enhanced dielectric and mechanical performance [21]. These effects explored further in the following sections.

3.2 Dielectric Properties

The dielectric properties of NCF reinforced with BTO, SNP, and CNT were assessed for potential applications in electronics and flexible antenna devices. The dielectric constant (ε') and dielectric loss (tan δ) were measured as a function of frequency, with the results shown in Figure 4. The NCF with BTO showed distinctly improved dielectric constants in the tested frequencies, due to the characteristically high permittivity of BTO (Figure 4a). This increase enables high electric energy storage, which is beneficial for antenna and capacitor applications necessitating high permittivity material [22]. The dielectric loss shows a dependence on frequency, as losses increases at low frequency and losses reduces at high frequencies,

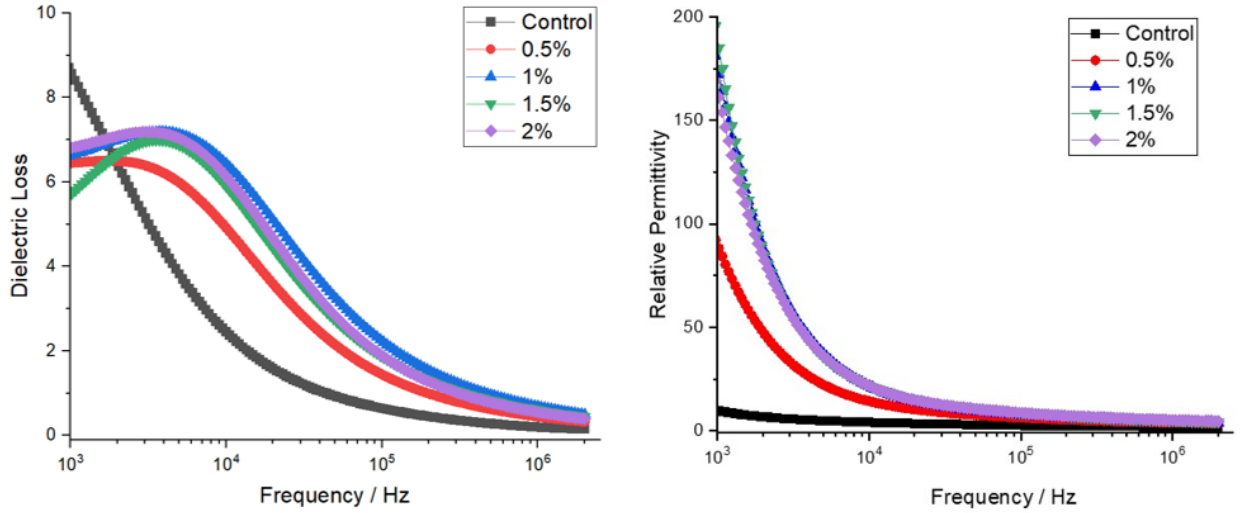

a. NCF with BTO nanofiller

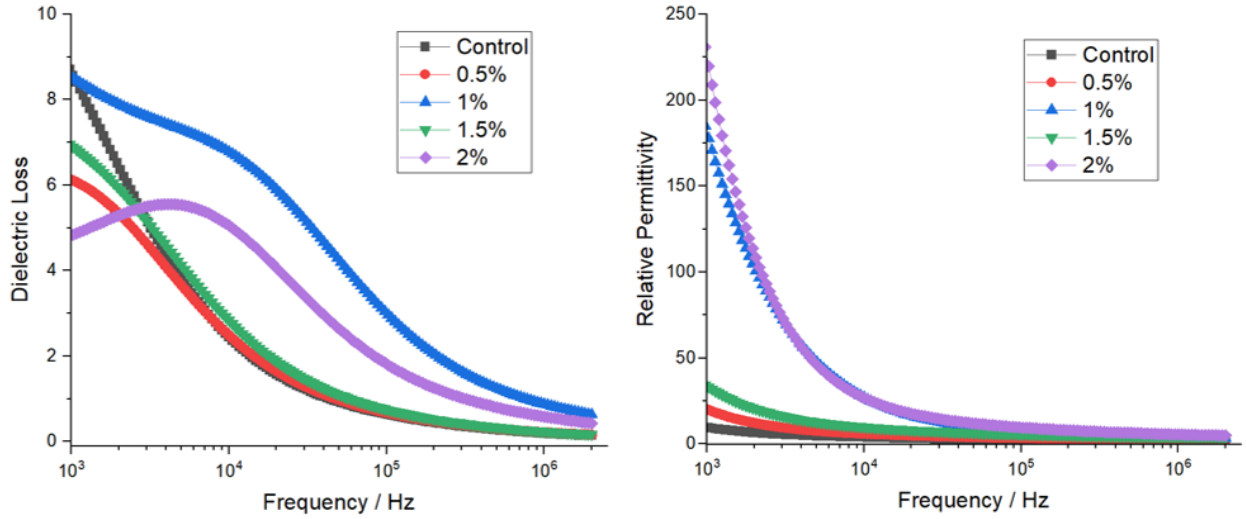

b. NCF with SNP nanofiller

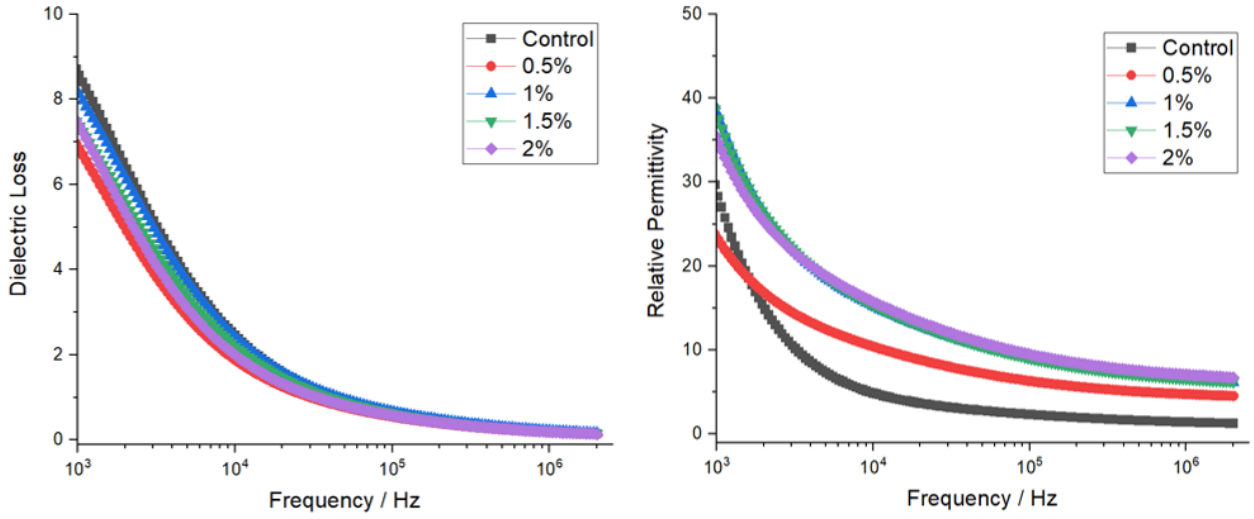

c. NCF with CNT nanofiller

Figure 4. Frequency-dependent dielectric properties of the NCF reinforced with (a) BTO, (b) SNP, and (c) CNT nanofillers.

this is an important consideration in high-frequency device [23].

However, the enhanced dielectric loss observed at higher BTO concentration indicates a trade-off with energy dissipation, potentially affect signal efficiency in high-frequency applications.

The incorporation of SNP resulted in moderate dielectric constant values (Figure 4b) accompanied by comparatively higher dielectric losses. The conductive nature of silver nanowires facilitates interfacial polarization, thereby improving charge storage but simultaneously inducing conduction losses. It also exhibits substantial change in dielectric loss with respect to frequency, show high losses at lower frequency that reduces as frequency rises, which directly influences the suitability for frequency-devices [24]. While this limits their use in low-loss antenna systems, the combined dielectric and conductive functionality make SNP-reinforced composites attractive for multifunctional devices such as transparent electrodes and flexible sensors [25, 26].

By contrast, NCF with CNT reinforcement exhibited a balanced dielectric profile: Moderate improvements in permittivity were achieved alongside consistently low dielectric loss values (Figure 4c). The high aspect ratio and strong interfacial interactions of CNTs promote dipolar polarization without inducing excessive conductive loss. It also maintains lower dielectric losses over a wide range of frequencies, highlights as a stable candidate for high-frequency applications [27]. This synergy makes the NCF-CNT composite a promising material for flexible antenna and electronic applications that require stable dielectric properties combined with mechanical flexibility [28]. These properties, combined with their mechanical flexibility, make CNT-reinforced CNF–PEO films particularly promising for wearable electronics and flexible antenna applications where both low loss and durability are required.

High-frequency measurements using the SPDR technique further confirmed these trends (Table 1). The reference materials displayed high permittivity values (3.61–4.57) and high Q-factors (1000–2600) compared with the nanocomposite films, which were thinner (0.27–1.29 mm) and exhibited permittivity in the 2.1–4.3 range. Among the nanofillers, CNT films consistently achieved the highest permittivity (3.67–4.25) with moderate dielectric loss (0.14–0.16), while BTO and SNP composites displayed more variable permittivity and higher losses. These findings support the conclusion that CNT provides the most effective reinforcement for balancing dielectric performance and energy efficiency in flexible, sustainable electronics.

3.3 Mechanical properties

The effect of nanofiller incorporation on the tensile properties of NCF was evaluated, with results summarised in Figure 5. Both tensile strength and elongation at break were compared against the control sample (NCF) to assess reinforcement efficiency and flexibility.

For films containing BTO, a trend of increasing tensile strength was observed with rising nanofiller content, particularly at 1.5–2.0% (Figure 5a). This behaviour can be attributed to the rigid, ceramic nature of BTO, which facilitates efficient stress transfer across the matrix-filler interface while restricting polymer chain mobility. Consequently, the films exhibited improved stiffness but reduced ductility at higher BTO loadings. Such reinforcement patterns, where strength is gained at the expense of elongation, are characteristic of ceramic nanofiller composites [29, 30], and was reported in other works where BTO was used as reinforcement in bio-composites [31].

Incorporation of SNP produced a moderate increase in tensile strength up to 1.5% concentration, followed by a decline at 2.0% (Figure 5b). This reduction is likely due to nanowire agglomeration, which introduces stress concentration points and weakens the composite structure. Elongation decreased significantly compared with BTO-filled films, reflecting the brittle nature of metallic nanowires. Although SNP can enhance mechanical strength through their high aspect ratio and conductivity, excessive loading undermines ductility and toughness [32, 33].

For CNT-reinforced films showed maximum tensile strength at 0.5% CNT loading (Figure 5c). The tensile strength found to be lower than BTO and SNP films. It suggests that incorporation of CNT provides reinforcement and it is insignificant to enhance ductility compared to BTO and SNP nanofillers [34, 35]]. Hence, mechanical properties suggest that, stiffness and reinforcement was achieved in NCF-BTO composite, NCF-SNP composite for stable reinforcement, and NCF-CNT composite for reinforcement at low concentrations without ductile improvement.

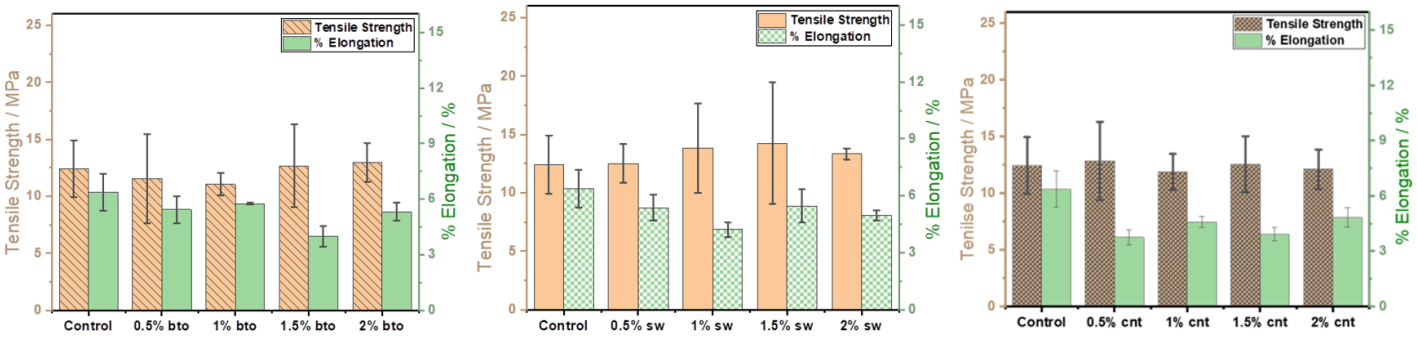

a. NCF with BTO nanofiller b. NCF with SNP nanofiller c. NCF with CNT nanofiller

Figure 5. Tensile strength and elongation at break of NFC reinforced with different nanofillers (a) BTO, (b) SNP, and (c) CNT.

Table 1. Dielectric properties of reference materials and NCF with various nanofillers measured using SPDR.

Samples	Frequency (MHz)	Q-factor	Thickness (mm)	Permittivity	Dielectric loss tangent (10^3)
Reference Material-I	1882.90	2600.00	1.53000	4.57357	1.78060e-002
Reference Material-II	1885.90	1000.00	1.63000	3.61357	6.16840e-002
CNF-PEQ (1:2)	1894.10	1900.00	0.27000	4.26280	1.52480e-001
NCF-0.5% BTO	1894.20	1800.00	0.40870	3.06894	1.49430e-001
NCF-1.0% BTO	1892.80	1100.00	1.28940	2.11387	1.20540e-001
NCF-1.5% BTO	1892.70	1000.00	0.57690	3.51025	1.76270e-001
NCF-2.0% BTO	1894.20	1800.00	0.57850	2.47015	1.31950e-001
NCF-0.5% SNP	1894.50	2200.00	0.37120	2.95488	1.35860e-001
NCF-1.0% SNP	1894.20	1900.00	0.49740	2.70513	1.31460e-001
NCF-1.5% SNP	1894.30	2000.00	0.47280	2.70821	1.30240e-001
NCF-2.0% SNP	1894.40	2100.00	0.47710	2.60977	1.26710e-001
NCF-0.5% CNT	1894.10	1800.00	0.27140	4.24614	1.61870e-001
NCF-1.0% CNT	1894.10	1800.00	0.28120	4.13414	1.60520e-001
NCF-1.5% CNT	1893.80	1700.00	0.37480	3.67595	1.44760e-001
NCF-2.0% CNT	1893.70	1700.00	0.39120	3.66655	1.39100e-001

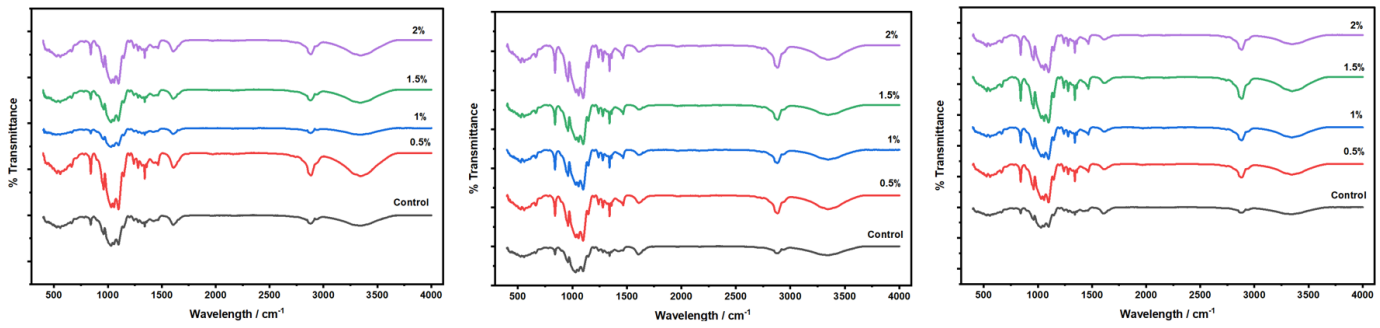

a. NCF with BTO nanofiller b. NCF with SNP nanofiller c. NCF with CNT nanofiller

Figure 6. FT-IR spectra of NCF with different nanofillers (a) BTO, (b) SNP, and (c) CNT.

3.4 FTIR Spectral Analysis

The FTIR spectra of NCF reinforced with BTO, SNP, and CNT revealed considerable molecular-level interactions and nanofiller incorporation, as shown by distinct shifts, enlargement, and the appearance of new absorption bands (Figure 6). The control NCF spectrum displayed the typical cellulose bands, including a broad O-H stretching vibration at 3340 cm^{-1}, C-H stretching at 2880 cm^{-1}, and a C-O-C stretching band near 1055 cm^{-1}. The presence of PEO contributed to enhanced hydrogen bonding within the polymer matrix, consistent with previous reports [36].

Upon addition of BTO in NCF, the O-H stretching band at ~3340 cm^{-1} broadened and decreased in intensity, suggesting disruption of intra- and intermolecular hydrogen bonding due to strong filler-matrix interactions. A new band appeared between

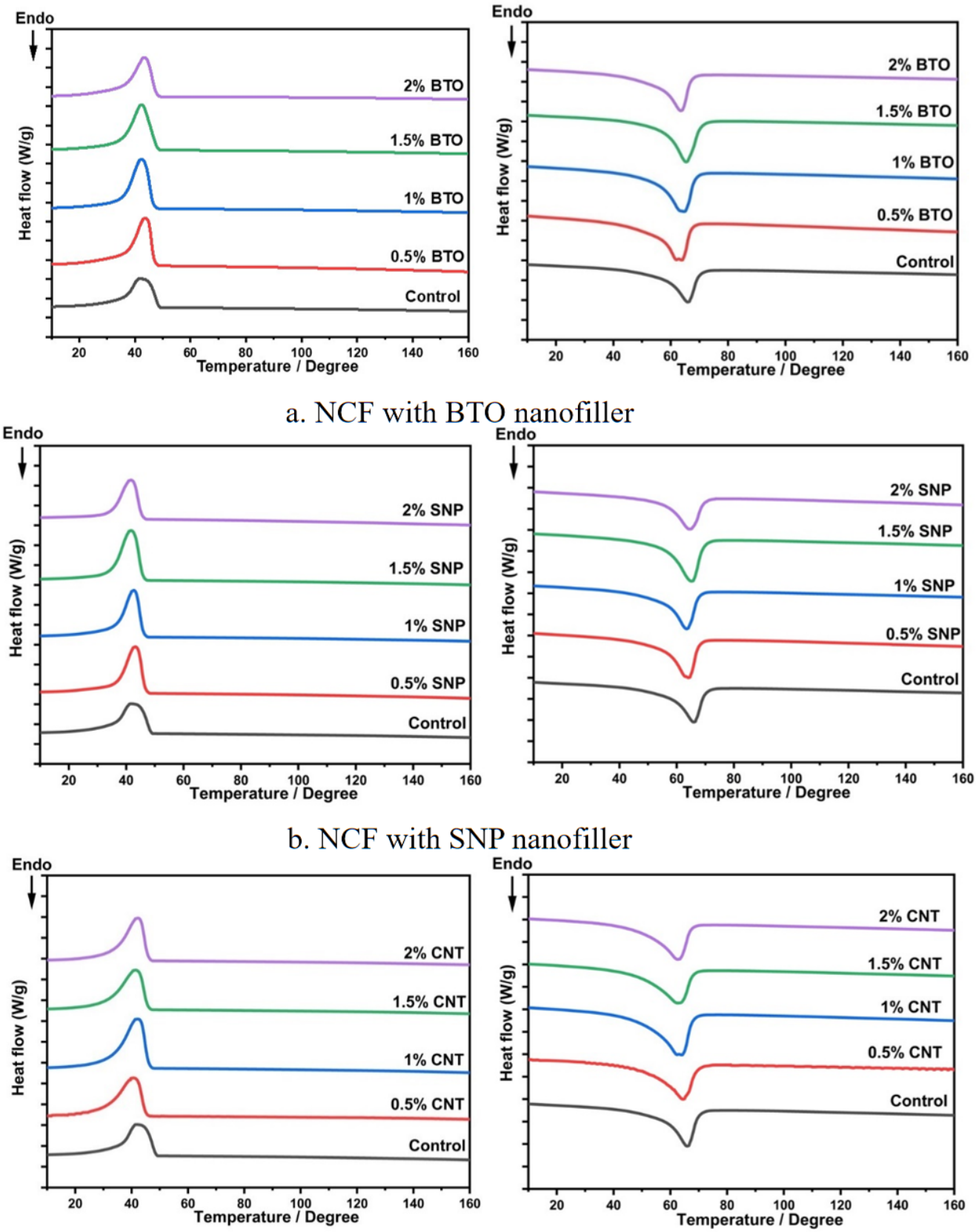

Figure 7. DSC thermograms of NCF with different nanofillers (a) BTO, (b) SNP, and (c) CNT.

580-630 cm^{-1}, corresponding to Ti-O stretching vibrations, confirming successful incorporation of BTO. Meanwhile, the diminished intensity of the C-O-C band at 1055 cm^{-1} indicated partial restriction of glycosidic linkage flexibility as filler concentration increased [37]. On addition of SNP nanofiller in NCF leads O-H band shifting and the occurrence of peak at near 1380 cm^{-1}, attributed to Ag-O bonding. The C-O-C vibrations at ∼1055 cm^{-1} equally decays in intensity, which signals modification of matrix from nanofiller incorporation. The silver concentration in NCF emphasises the changes in spectra [38,39]. In the case of CNT, the O-H band exhibited significant broadening, and a new peak emerged at ∼1550–1600 cm^{-1}, corresponding to CNT vibrational modes. These effects became more pronounced at ≥0.5 % CNT loading, demonstrating disruption of crystalline ordering and the formation of strong matrix-nanotube interactions. The resulting spectral changes confirm the establishment of robust conductive networks and physical reinforcement within the composites [40, 41].

3.5 Differential Scanning Calorimetry

Differential Scanning Calorimetry (DSC) analysis was performed to evaluate melting (T_m) and crystallisation (T_c) behaviour of the nanocomposites (Figure 7). All samples exhibited two distinct transitions: an exothermic crystallisation peak at 41 °C and an endothermic melting peak at 65 °C, consistent with the PEO crystalline phase.

The incorporation of BTO and SNP has no impact on the thermal properties of NCF samples, with T_m and T_c similar with or without fillers (within the range of error, ± 1°C). This suggests that BTO and SNP are not significantly disrupting the crystalline structure of PEO-CNF matrix. By contrast, CNT reinforced composites exhibited a reduction in crystallisation temperature and melting temperature compared to the control sample. The addition of CNT induces a decrease of 3°C in T_c, from 43°C down to 40°C, and in T_m, from 65°C down to 62°C, respectively. Jin et al. [42] found similar behaviour with the incorporation of CNT with pure PEO matrix. This shift towards lower temperature can be attributed to the disruption of the crystalline part in PEO-CNF matrix. The presence of CNT may disrupt the alignment of PEO chains, leading to a further decrease in crystallinity and a reduction in the thermal energy needed for melting.

4 Conclusion

This study exhibited the effective fabrication of biodegradable nanocomposite films composed of WH-derived nanocellulose blended with PEO and reinforced with nanofillers (BTO, SNP, CNT). The reinforcement of BTO nanofillers significantly improves dielectric permittivity, making these NCF extremely appropriate for applications demanding high dielectric constants, such as dielectric resonators, and capacitive devices, though with a moderate rise in dielectric loss. NCF with SNP offer multifunctional properties combining dielectric behaviour and conductivity, perfect for flexible electronic sensors and electrodes despite high dielectric loss. NCF with CNT strike an optimum balance by provided that mechanical flexibility and low dielectric loss, favouring applications in wearable and flexible antenna technologies. Mechanically, BTO imparts higher strength and stiffness with reduced flexibility, while SNP and CNT offer diverse trade-offs between ductility and strength. The molecular interaction between NCF and nanofillers revealed the enhanced mechanical and electrical properties. The DSC analysis noted that BTO and SNP nanofillers as reinforcement did not influence the thermal behaviour of CNF, conserving the melting transitions and crystallization of the matrix. Whereas, incorporation of CNT interrupted the crystalline arrangement of PEO in CNF, leading to reduced melting temperature and crystallization. This study highlights the possible of valorization of an invasive biomass into high-performance, eco-friendly materials, for next-generation green flexible electronics. Future work would focus on optimizing the dispersion of nanofiller and hybrid nanocomposite formulations to tailor properties for specific electronic device applications.

Data Availability Statement

Data will be made available on request.

Funding

This work was supported without any funding.

Conflicts of Interest

The authors declare no conflicts of interest.

Ethical Approval and Consent to Participate

Not applicable.

References

[1] Dulal, M., Modha, H. R. M., Liu, J., Islam, M. R., Carr, C., Hasan, T., ... & Karim, N. (2025). Sustainable, Wearable, and Eco-Friendly Electronic Textiles. *Energy & Environmental Materials*, *8*(3), e12854. [CrossRef]

[2] Moshood, T. D., Nawanir, G., Mahmud, F., Mohamad, F., Ahmad, M. H., & AbdulGhani, A. (2022). Sustainability of biodegradable plastics: New problem or solution to solve the global plastic pollution?. *Current Research in Green and Sustainable Chemistry, 5*, 100273. [CrossRef]

[3] Thomas, B., Raj, M. C., B, A. K., Joy, J., Moores, A., Drisko, G. L., & Sanchez, C. (2018). Nanocellulose, a versatile green platform: from biosources to materials and their applications. *Chemical Reviews, 118*(24), 11575-11625. [CrossRef]

[4] Ibanez Labiano, I., Arslan, D., Ozden Yenigun, E., Asadi, A., Cebeci, H., & Alomainy, A. (2021). Screen printing carbon nanotubes textiles antennas for smart wearables. *Sensors, 21*(14), 4934. [CrossRef]

[5] Packiam, K. K., Murugesan, B., Kaliyannan Sundaramoorthy, P. M., Srinivasan, H., & Dhanasekaran, K. (2022). Extraction, purification and characterization of nanocrystalline cellulose from Eichhornia crassipes (Mart.) solms: a common aquatic weed water hyacinth. *Journal of Natural Fibers, 19*(14), 7424-7435. [CrossRef]

[6] Ghamari, M., Sun, D., Dai, Y., See, C. H., Yu, H., Edirisinghe, M., & Sundaram, S. (2024). Valorization of diverse waste-derived nanocellulose for multifaceted applications: A review. *International Journal of Biological Macromolecules, 280*, 136130. [CrossRef]

[7] Vijayakumary, P., Manisha, R. B., Meenakshi, P., Parimala, D. R., Subramanian, P., Sriramajayam, S., ...& Ramesh, D. (2024). Conversion of sugarcane bagasse into cellulose, carboxymethyl cellulose, and polymer membrane electrolyte and their characterization. *Plant Science Today, 11*, 5874. [CrossRef]

[8] Chaiwarit, T., Chanabodeechalermrung, B., Kantrong, N., Chittasupho, C., & Jantrawut, P. (2022). Fabrication and evaluation of water hyacinth cellulose-composited hydrogel containing quercetin for topical antibacterial applications. *Gels, 8*(12), 767. [CrossRef]

[9] Pantamanatsopa, P., Ariyawiriyanan, W., & Ekgasit, S. (2023). Production of cellulose nanocrystals suspension with high yields from water hyacinth. *Journal of Natural Fibers, 20*(1), 2134266. [CrossRef]

[10] Nandi, S., Kerur, S. S., & Dhanalakshmi, S. (2024). Electrical and dielectric properties of polymer-metal hybrid nanocomposites-A short review. *Diffusion Foundations and Materials Applications, 35*, 1-13. [CrossRef]

[11] Farzin, M. A., Naghib, S. M., & Rabiee, N. (2024). Advancements in bio-inspired self-powered wireless sensors: Materials, mechanisms, and biomedical applications. *ACS Biomaterials Science & Engineering, 10*(3), 1262-1301. [CrossRef]

[12] AL-Oqla, F. M. (2020). Biocomposites in advanced biomedical and electronic systems applications. In *Composites in biomedical applications* (pp. 49-70). CRC Press. [CrossRef]

[13] Asrofi, M., Abral, H., Kasim, A., Pratoto, A., Mahardika, M., Park, J. W., & Kim, H. J. (2018). Isolation of nanocellulose from water hyacinth fiber (WHF) produced via digester-sonication and its characterization. *Fibers and Polymers, 19*(8), 1618-1625. [CrossRef]

[14] Uyor, U. O., Popoola, A. P. I., & Popoola, O. M. (2023). Flexible dielectric polymer nanocomposites with improved thermal energy management for energy-power applications. *Frontiers in Energy Research, 11*, 1114512. [CrossRef]

[15] Sun, D., Onyianta, A. J., O'Rourke, D., Perrin, G., Popescu, C. M., Saw, L. H., ...& Dorris, M. (2020). A process for deriving high quality cellulose nanofibrils from water hyacinth invasive species. *Cellulose, 27*(7), 3727-3740. [CrossRef]

[16] Krupka, J., Clarke, R. N., Rochard, O. C., & Gregory, A. P. (2000, May). Split post dielectric resonator technique for precise measurements of laminar dielectric specimens-measurement uncertainties. In *13th International Conference on Microwaves, Radar and Wireless Communications. MIKON-2000. Conference Proceedings* (Vol. 1, pp. 305-308). IEEE. [CrossRef]

[17] Yaw, K. C. (2012). *Measurement of dielectric material properties*. Application Note. Rohde & Schwarz, 1-35.

[18] Sehaqui, H., Zhou, Q., & Berglund, L. A. (2011). High-porosity aerogels of high specific surface area prepared from nanofibrillated cellulose (NFC). *Composites Science and Technology, 71*(13), 1593-1599. [CrossRef]

[19] Dang, Z. M., Yuan, J. K., Zha, J. W., Zhou, T., Li, S. T., & Hu, G. H. (2012). Fundamentals, processes and applications of high-permittivity polymer–matrix composites. *Progress in Materials Science, 57*(4), 660-723. [CrossRef]

[20] Moon, R. J., Martini, A., Nairn, J., Simonsen, J., & Youngblood, J. (2011). Cellulose nanomaterials review: structure, properties and nanocomposites. *Chemical Society Reviews, 40*(7), 3941-3994. [CrossRef]

[21] Yang, L., Qiu, J., Ji, H., Zhu, K., & Wang, J. (2014). Enhanced dielectric and ferroelectric properties induced by TiO2@ MWCNTs nanoparticles in flexible poly (vinylidene fluoride) composites. *Composites Part A: Applied Science and Manufacturing, 65*, 125-134. [CrossRef]

[22] Khosroshahi, F. H., Kordi, F., & Tohidian, M. (2025). Preparation of cross-linked sponge with piezoelectric properties based on low density polyethylene/poly (ethylene-co-vinyl acetate) and barium titanate:

Relationship between mechanical properties, and cell structure with piezoelectric coefficients. *Polymers for Advanced Technologies, 36*(2), e70084. [CrossRef]

[23] Mabrouki, A. E., Messaoudi, O., Dhahri, A., Azhary, A., Mansouri, M., & Alfhaid, L. (2025). Investigation of the frequency-dependent dielectric properties of the as-prepared LaNiO3/Co3O4 nanocomposites. *ACS Omega, 10*(22), 22701-22710. [CrossRef]

[24] Durai, S. V., & Kumar, E. (2020). Frequency-dependent impedance, modulus and dielectric studies of polyaniline/manganese dioxide nanocomposites. *Journal of Ovonic Research, 16*(3), 173-180.

[25] Sayin, G., Kurnaz, S., Tokeşer, E. A., Seydioğlu, T., & Öztürk, Ö. (2025). Frequency-dependent dielectric and impedance properties of TPU-graphene nanocomposites. *Sensors and Actuators A: Physical*, 116938. [CrossRef]

[26] Chen, Y., Carmichael, R. S., & Carmichael, T. B. (2019). Patterned, flexible, and stretchable silver nanowire/polymer composite films as transparent conductive electrodes. *ACS Applied Materials & Interfaces, 11*(34), 31210-31219. [CrossRef]

[27] Zeraati, A. S., Arjmand, M., & Sundararaj, U. (2017). Silver nanowire/MnO2 nanowire hybrid polymer nanocomposites: materials with high dielectric permittivity and low dielectric loss. *ACS Applied Materials & Interfaces, 9*(16), 14328-14336. [CrossRef]

[28] Zhou, Y., Bayram, Y., Du, F., Dai, L., & Volakis, J. L. (2010). Polymer-carbon nanotube sheets for conformal load bearing antennas. *IEEE Transactions on Antennas and Propagation, 58*(7), 2169-2175. [CrossRef]

[29] Liu, J., He, X., Wang, F., Zhou, X., & Li, G. (2021). Dielectric and mechanical properties of polycaprolactone/nano-barium titanate piezoelectric composites. *Plastics, Rubber and Composites, 50*(6), 299-306. [CrossRef]

[30] Turcanu, G., Stoica, I., Albu, R. M., Varganici, C. D., Avadanei, M. I., Barzic, A. I., …& Buscaglia, M. T. (2025). Design of polysaccharide-based nanocomposites for eco-friendly flexible electronics. *Polymers, 17*(12), 1612. [CrossRef]

[31] Das Lala, S., Deoghare, A. B., & Chatterjee, S. (2018). Effect of reinforcements on polymer matrix bio-composites–an overview. *Science and Engineering of Composite Materials, 25*(6), 1039-1058. [CrossRef]

[32] Sha, Z., Cheng, X., Islam, M. S., Sangkarat, P., Chang, W., Brown, S. A., …& Wang, C. H. (2023). Synergistically enhancing the electrical conductivity of carbon fibre reinforced polymers by vertical graphene and silver nanowires. *Composites Part A: Applied Science and Manufacturing, 168*, 107463. [CrossRef]

[33] Lee, I., Lee, J., Ko, S. H., & Kim, T. S. (2013). Reinforcing Ag nanoparticle thin films with very long Ag nanowires. *Nanotechnology, 24*(41), 415704. [CrossRef]

[34] Wang, X., & Wu, P. (2018). Fluorinated carbon nanotube/nanofibrillated cellulose composite film with enhanced toughness, superior thermal conductivity, and electrical insulation. *ACS Applied Materials & Interfaces, 10*(40), 34311-34321. [CrossRef]

[35] Sadasivuni, K. K., Saha, P., Adhikari, J., Deshmukh, K., Ahamed, M. B., & Cabibihan, J. J. (2020). Recent advances in mechanical properties of biopolymer composites: a review. *Polymer Composites, 41*(1), 32-59. [CrossRef]

[36] Azeez, S., & Shenbagaraman, R. (2025). Fourier transform infrared spectroscopy in characterization of bionanocomposites. In *Characterization Techniques in Bionanocomposites* (pp. 209-227). Woodhead Publishing. [CrossRef]

[37] Atta, M. R., Algethami, N., Farea, M. O., Alsulami, Q. A., & Rajeh, A. (2022). Enhancing the structural, thermal, and dielectric properties of the polymer nanocomposites based on polymer blend and barium titanate nanoparticles for application in energy storage. *International Journal of Energy Research, 46*(6), 8020-8029. [CrossRef]

[38] Sadeghi, E., Taghavi, R., Hasanzadeh, A., & Rostamnia, S. (2024). Bactericidal behavior of silver nanoparticle decorated nano-sized magnetic hydroxyapatite. *Nanoscale Advances, 6*(24), 6166-6172. [CrossRef]

[39] El Idrissi El Hassani, C., Daoudi, H., El Achaby, M., & Kassab, Z. (2023). Biomedical applications of chitosan-based nanostructured composite materials. In *Chitosan Nanocomposites: Bionanomechanical Applications* (pp. 81-107). Springer Nature Singapore. [CrossRef]

[40] Shah, S. A., Ali, H., Inayat, M. I., E. Mahmoud, E., Al Garalleh, H., & Ahmad, B. (2024). Effect of carbon nanotubes and zinc oxide on electrical and mechanical properties of polyvinyl alcohol matrix composite by electrospinning method. *Scientific Reports, 14*(1), 28107. [CrossRef]

[41] Sahoo, N. G., Cheng, H. K. F., Li, L., Chan, S. H., Judeh, Z., & Zhao, J. (2009). Specific functionalization of carbon nanotubes for advanced polymer nanocomposites. *Advanced Functional Materials, 19*(24), 3962-3971. [CrossRef]

[42] Jin, F. L., & Park, S. J. (2011). A review of the preparation and properties of carbon nanotubes-reinforced polymer composites. *Carbon Letters, 12*(2), 57-69. [CrossRef]

Gitanjali Jothiprakash serves as an associate staff at Edinburgh Napier University. She holds a B.Tech in Energy and Environmental Engineering and earned her M.Tech and Ph.D. in Bioenergy from Tamil Nadu Agricultural University with a University Gold Medal. Her research focuses on renewable energy and sustainable bioresource utilization. (Email: jogitanjali@gmail.com)

Dongyang Sun is an academic staff at Edinburgh Napier University, specializing in nanomaterials and electrohydrodynamic atomisation (EHDA) for printing applications. He completed his Ph.D. in Materials at the University of London and has contributed to patented research on nanocellulose production. His expertise also includes advanced materials characterization and wood science. (Email: D.Sun@napier.ac.uk)

Peter Adonteng is a Senior Professional Engineer (SPE) with the Ghana Institution of Engineers (GhIE) and a postgraduate student in Advanced Materials Engineering at Edinburgh Napier University, UK. He has extensive professional experience in materials development, process optimization, metallurgy and project management, with research interests in sustainable engineering solutions, energy engineering and advanced nanotechnology applications. (Email: 40708886@live.napier.ac.uk)

Chan Hwang See is Professor at Edinburgh Napier University with expertise in IoT, wireless sensor networks, antennas, and microwave circuits. He earned his B.Eng (Hons) and Ph.D. from the University of Bradford, UK, and previously served as Head of Electrical Engineering & Mathematics. His research spans IoT, wireless sensor networks, antennas, microwave circuits, wireless power transfer & computational electromagnetics. (Email: C.See@napier.ac.uk)

Elsa Lasseuguette is a Laboratory Technician at Edinburgh Napier University. She previously worked at the University of Edinburgh, where her research focused on developing advanced membrane technologies for CO_2 capture, gas separation, and nanofiltration. With a Ph.D. in Materials Science/Engineering from INPG–CNRS, France, she brings expertise in polymer characterization and sustainable materials development. (Email: E.Lasseuguette@napier.ac.uk)

Zhilun Lu is an Assistant Professor in the School of Chemical and Process Engineering at the University of Leeds. He holds a Ph.D. in Materials Science from the University of Sheffield, where he specialised in functional ceramics and defect chemistry. His research focuses on electroceramics, ferroelectrics, and thermoelectrics, with applications in sustainable energy and electronic devices. (Email: Z.Lu@leeds.ac.uk)

Ramesh Desikan is Professor and Head of the Department of Renewable Energy Engineering at Tamil Nadu Agricultural University, India. Undergone post-doctoral training on algae biofuels at Durban University of Technology, South Africa. He has experience in synthesis of biofuels, biochemicals and biomaterials from agro residues, and sustainable energy technologies. (Email: rameshd@tnau.ac.in)

Subburamu Karthikeyan is a Professor (Microbiology) and leads the Centre for Post-Harvest Technology, as the Quality Manager of the NABL-accredited Food Quality Testing Laboratory at Tamil Nadu Agricultural University, Coimbatore. He has post-doctoral experience in algal systems for wastewater treatment and biofuel production and actively contributes to research, teaching, and funded projects. His research interests include biomass refining, fermentation, anaerobic microbiology, and carbon sequestration within multidisciplinary agriculture. (Email: skarthy@tnau.ac.in)

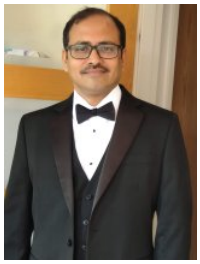

Senthilarasu Sundaram is a Professor in the School of Computing, Engineering, and Digital Technologies at Teesside University. His passion towards energy and sustainability in the energy sector has started during his pre-doctoral research course (MPhil in Applied Physics) which led to PhD in organic solar cell materials. His expertise spans solar resource assessment, modelling, and sustainable energy systems. His research focuses on dye-sensitised and perovskite solar cells, energy storage, building integration, and low-carbon applications. (Email: s.sundaram@tees.ac.uk)